Optical and Quantum Electronics (2020) 52:495
https://doi.org/10.1007/s11082-020-02573-5

Role of external fields on the nonlinear optical properties of a n-type asymmetric δ-doped double quantum well

Aysevil Salman Durmuslar[1] · Miguel Eduardo Mora-Ramos[2,3] · Fatih Ungan[4]

Received: 20 July 2020 / Accepted: 28 September 2020
© Springer Science+Business Media, LLC, part of Springer Nature 2020

Abstract
The effects of in-growth applied electric fields and in-plane (x-oriented) magnetic fields on the nonlinear optical rectification (NOR), second harmonic generation (SHG) and third harmonic generation (THG) of n-type asymmetric double δ-doped GaAs quantum well are theoretically investigated. One-dimensional Schrödinger equation is solved by considering effective mass and parabolic band approximations to obtain subband energy levels and their related wave functions. The variations in the NOR, SHG and THG coefficients are determined by using the iterative solutions of the compact density matrix approach. Obtained results indicate that the applied electric field leads to optical red-shift on NOR, SHG and THG coefficients while the magnetic field causes optical blue-shift on that coefficients. Hence we can conclude that applied electromagnetic fields can be used to tune optical properties of devices working within the region of infrared electromagnetic spectrum.

Keywords δ-Doped double quantum well · Nonlinear optical response · Electric field · Magnetic field

1 Introduction

In the recent years there is a great interest on the electronic and the optical properties of low-dimensional systems such as quantum wells (QWs), due to their device applications. Such systems can be fabricated with various confining potential geometries thanks to crystal growth techniques, such as molecular beam epitaxy and metal-organic chemical vapor deposition. Besides, it is possible to manipulate the band confinement potentials via structure parameters such as well width, barrier width, doping concentration or external

✉ Aysevil Salman Durmuslar
asdurmuslar@pirireis.edu.tr

[1] Department of Naval Architecture and Marine Engineering, Faculty of Engineering, Piri Reis University, 34940 Istanbul, Turkey

[2] Centro de Investigación en Ciencias-IICBA, Universidad Autónoma del Estado de Morelos, Av. Universidad 1001, Col. Chamilpa, 62209 Cuernavaca, Morelos, Mexico

[3] Facultad de Ciencias Básicas, Universidad de Medellín, Medellín, Colombia

[4] Department of Optical Engineering, Faculty of Technology, Sivas Cumhuriyet University, Sivas, Turkey

probes such as intense laser field, electric and magnetic fields. The shape of confinement potential determines the electronic structures of quantum systems and, therefore, acts on the transitions between intersubband (ISB) energy levels. The variations in the ISB transitions affect the electric dipole moment matrix elements of these state wave functions and result in changes on linear and nonlinear optical properties. Forming asymmetric QWs or breaking the symmetry of confinement potential is crucial to get significant second order susceptibilities such as nonlinear optical rectification (NOR) and second harmonic generation (SHG).

The so-called δ-doped semiconductor heterostructures represent a typical confinement profile with its narrow V-shaped geometry. δ-doping technique is frequently preferred due to its potential implementations in the optoelectronic devices such as high-power field effect transistors, infrared lasers, infrared modulators and far-infrared detectors. This technique localizes a large amount of impurities—that ionize within very thin layers—and leads to the appearance of a quasi-two-dimensional electron gas system with high-density. Also, the technique produces a higher electronic mobility by decreasing the doped layer thickness (Kozuka et al. 2010) and forms narrow, sharp doping profiles. δ-doped structures exhibit strong confinement effect and small subband energy separations compared to that of bulk semiconductor materials. As known, application of electric and magnetic fields to QWs results in modifications in the confinement potential and, so, in the energy levels. In this wise, optical properties can be tuned and controlled as desired. For these reasons, the effect of applied electric and magnetic fields onto the linear and nonlinear optical properties of δ-doped QWs is studied by many researchers (Rodíguez-Magdaleno et al. 2014; Dakhlaoui and Nefzi 2019; Martínez-Orozco et al. 2016; Ozturk 2009; Yildirim and Tomak 2006; Martínez-Orozco et al. 2017). In the works Rodíguez-Magdaleno et al. (2014), Dakhlaoui and Nefzi (2019), Martínez-Orozco et al. (2016), Ozturk (2009), Yildirim and Tomak (2006)), the effects of magnetic and electric field on the optical absorption coefficients and relative refractive indexes, associated with electron transitions in the δ-doped QWs were investigated. Martinez-Orozco and co-workers (2017) performed a study to realize on the influence of an in-plane constant magnetic field to the NOR, SHG and third harmonic generation (THG) coefficients, in the case of asymmetric double δ-doped GaAs QWs. They reported that these susceptibilities can be controlled by magnetic field at the far-infrared region. The studies to examine the effect of electric and/or magnetic field on the NOR, SHG and THG coefficients for several types of QWs are summarized as below: Rosencher et al. (1989) carried out the first experimental study on NOR susceptibility for asymmetric multi QWs. Karabulut and coworkers (2005) investigated the variations on NOR coefficients in the presence of electric field for semi-parabolic QWs. The effect of electric fields on NOR coefficients is studied for parabolic QWs by Guo and Gu (1993) and for double triangular QWs by Chen et al. (2008). Karabulut et al. (2011) theoretically examined the influence of independent or combined application of electric field, magnetic field and hydrostatic pressure on the NOR susceptibility and optical absorption for an asymmetric double QW. Karimi and Keshavarz (2012) studied the responses of NOR coefficient in the presence of electric field, magnetic field and also hydrostatic pressure. Influences of electric field together with well and barrier width are studied for a symmetric coupled QW by Liu et al. (2018). A study on both NOR and SHG coefficients is performed by Liu et al. (2016) for asymmetrical Gaussian potential QW with applied magnetic field. Other theoretical investigations on the SHG susceptibility in the presence of applied electric field have been carried out by Tsang et al. (1988), for an infinite QW, and by Zhang and Xie (2003), for the parabolic and semi-parabolic QWs. In their study, Zhang and Xie reported that semi-parabolic QWs exhibit greater SHG enhancement and susceptibility

than parabolic QWs in the presence of electric field. Besides, Panda et al. (2019) investigated the variation of NOR, SHG and THG coefficients with the effect of electric field for $In_xGa_{1-x}N/GaN$ hexagonal single QW and concluded electric field leads a blue-shift on the mentioned coefficients. To sense the effects of electric and magnetic fields together with intense laser field on the NOR, SHG and THG coefficients, a study was performed by Mora-Ramos and co-workers (2012). They reported that these responses and related energy levels, as well as the electric dipole matrix elements, are considerably influenced by applied fields. Restrepo et al. (2017) carried out a research on the geometrical parameter that determines the width of Morse QW under applied electromagnetic fields. In that study, the authors concluded that peak amplitudes and peak positions of SHG and THG vary as a result of applied electric and magnetic fields and also well width. Zhang and Xie (2004) once again analyzed the semiparabolic QW to examine the behavior of THG coefficients in the presence of an electric field. In addition, there are some studies to state the effect of electric and magnetic field on THG in quantum wires. Wang (2005) studied the influence of electric fields in the case of cylindrical parabolic quantum wires, while Rezaei and Karimi (2012) worked on the effect of magnetic field for coaxial cylindrical quantum well wires; and Guo et al. (2001) examined magnetic field effect for double layered quantum wires. On the other hand, there are some other researches aimed at determining the effect of static electric and magnetic field on NOR coefficients in several types of quantum dots (Li et al. 2008, 2014; Chen et al. 2012; Baskoutas et al . 2007; Zhang et al. 2009a; Giraldo-Tobon et al. 2015; Vaseghi et al. 2015), on SHG coefficients in parabolic quantum dot Li et al. (2007), and on THG coefficients in various shapes of quantum dots (Vaseghi et al. 2015; Zhang et al. 2009b; Shao et al. 2011; Kirak and Altinok 2012; Ganguly et al. 2016).

In the present work, we use the effective mass and parabolic band approximations to obtain the electron subband energy levels and corresponding wave functions of n-type asymmetric δ-doped double QW. The calculation of optical properties is carried out by using the respective expressions that arise from the iterative solution of compact density matrix equation. Up to our knowledge there is only one study—performed by Martínez-Orozco et al. (2017)—on the NOR, SHG and THG susceptibilities of asymmetric double δ-doped QWs in the presence of magnetic fields. So, we aim at to examine the effect of electric field and also the magnetic field on the NOR, SHG and THG coefficients in a asymmetric double δ-doped QW with different values of the ionized impurity density as reported in the literature. The paper continues with the theoretical model given in Sect. 2. The results and related discussions are presented in Sect. 3. Section 4 includes a brief summary and main conclusion.

2 Theoretical model

We shall make a theoretical investigation for an asymmetric double n-type δ-doped GaAs quantum wells (ADDDQWs) in the presence of static electric and magnetic fields. Within the framework of effective mass and parabolic band approaches, the three-dimensional Hamiltonian of a confined electron under the influence of external electric and magnetic fields is given in the following form:

$$H = -\frac{1}{2m^*}\left(\mathbf{p} + \frac{e}{c}\mathbf{A}(\mathbf{r})\right)^2 + V_{TF}(\mathbf{r}) + e\mathbf{F}\cdot\mathbf{r} \tag{1}$$

where m^* is the electron effective mass, $\mathbf{p}$ is the momentum operator, e is the electron charge and c is the speed of light in vacuum. Here, we assume the QW is grown along the z-axis and the magnetic field of strength B is applied in-plane; in this case along x-direction as $\mathbf{B} = B\hat{\mathbf{x}}$. The corresponding vector potential of the magnetic field in the Landau gauge is given by $\mathbf{A}(\mathbf{r}) = -Bz\hat{\mathbf{y}}$ while static electric field of strength F is applied along the growth direction as $\mathbf{F} = F\hat{\mathbf{z}}$. $V_{TF}(\mathbf{r})$ represents the confinement potential of double δ-doped QW, written within the local density Thomas-Fermi (TF) approximation.

With that assumptions the Hamiltonian of an electron confined in QW grown in the z-direction can be reduced to one-dimensional form as

$$H_z = -\frac{\hbar^2}{2m^*}\frac{d^2}{dz^2} + \frac{e^2B^2}{2m^*c^2}z^2 + V_{TF}(z) + eFz. \tag{2}$$

And the expression of confinement potential can be written as below by adopting analytical expression (Ioriatti 1990) to our problem:

$$V_{TF}(z) = -\frac{\alpha^2}{(\alpha|z - L_w/2 + z_{0R}|)^4} - \frac{\alpha^2}{(\alpha|z - L_w/2 + z_{0L}|)^4}. \tag{3}$$

where $\alpha = e^2(2m^*)^{3/2}/(15\pi\varepsilon\hbar^3)$, $z_{0L} = [(2\varepsilon\alpha^3)/(\pi e^2 N_{2d}^L)]^{1/5}$, $z_{0R} = [(2\varepsilon\alpha^3)/(\pi e^2 N_{2d}^R)]^{1/5}$ are the local-density TF parameters. L_w indicates the distance between the right- and left-side δ-doped planes and ε is the static dielectric constant of the host material. In addition, N_{2d}^L and N_{2d}^R represent the density of ionized impurities in the left- and right-hand side of δ -doped layers, respectively.

To obtain the energy levels and the wave functions we solved the one-dimensional Schrödinger equation, $H_z\phi(z) = E_z\phi(z)$, with the use of the diagonalization method (Xia and Fan 1989). This method offers to express single electron wave function $\phi(z)$ in terms of complete set of orthonormal functions as,

$$\phi(z) = \sqrt{\frac{2}{L_\infty}}\sum_n C_n \sin\left(\frac{n\pi z}{L_\infty} + \frac{n\pi}{2}\right). \tag{4}$$

These functions are no other than the wave functions of a potential well of infinite barriers and width L_∞. C_n is the expansion coefficient and n is a non-negative integer number.

By obtaining energy levels and corresponding wave functions, we get detailed information about ISB transitions and dipole moment matrix elements associated to these subbands. Afterwards we make use of the analytical expressions for the NOR, SHG and THG coefficients. In order to obtain THG coefficients one need four energy levels while three (two) energy levels are sufficient for SHG (NOR). The expressions for the calculation of NOR, SHG and THG coefficients can be written respectively as (Martínez-Orozco et al. 2017; Shao et al. 2011; Rosencher and Bois 1991; Yu and Wang 2011):

$$\chi_0^{(2)} = \frac{4e^3\rho_{01}}{\varepsilon_0\hbar^2}M_{01}^2\delta_{01}\frac{\omega_{10}^2(1+\Gamma_2/\Gamma_1) + (\omega^2+\Gamma_2^2)(\Gamma_2/\Gamma_1 - 1)}{[(\omega_{10}-\omega)^2+\Gamma_2^2][(\omega_{10}+\omega)^2+\Gamma_2^2]} \tag{5}$$

$$\chi_{2\omega}^{(2)} = \frac{e^3\rho_{01}}{\varepsilon_0\hbar^2}\frac{M_{01}M_{12}M_{20}}{(\omega-\omega_{10}-i\Gamma_3)(2\omega-\omega_{20}-i\Gamma_3)} \tag{6}$$

$$\chi_{3\omega}^{(3)} = \frac{e^4 \rho_{03}}{\varepsilon_0 \hbar^3} \frac{M_{01} M_{12} M_{23} M_{30}}{(\omega - \omega_{10} - i\Gamma_3)(2\omega - \omega_{20} - i\Gamma_3)(3\omega - \omega_{30} - i\Gamma_3)} \tag{7}$$

where $\omega_{ij} = (E_i - E_j)/\hbar$, $(i,j = 0,1,2,3)$ is the transition frequency between the initial (j) and final (i) state and $M_{ij} = \langle \varphi_i | z | \varphi_j \rangle$, are off-diagonal matrix elements of the dipole moment operator and δ_{10} is expressed as $|M_{00} - M_{11}|$. The term $\Gamma_k = 1/T_k$, being $(k = 1,2,3)$, is the relaxation rate associated with transition lifetime of the electrons, and the quantity $\rho_{0i} = \rho_0 - \rho_i$, $(i = 1,3)$ represents the difference between temperature-dependent density of electrons involved in transition and it is given by

$$\rho_{0i} = \frac{m^* k_B T}{\pi \hbar^2 L_w} \ln \left[\frac{1 + \exp[(E_F - E_0)/k_B T]}{1 + \exp[(E_F - E_i)/k_B T]} \right]. \tag{8}$$

Here E_F is the Fermi energy, k_B is the Boltzmann constant, T is the temperature, and L_w is the effective well width of system. Finally, at the low temperatures where the thermal energy $K_B T$ is much smaller than all the energy differences between levels $(E_F - E_i)$, the difference of electron densities between excited levels and ground level is given by

$$\rho_{0i} = \frac{m^*}{\pi \hbar^2 L_w} (E_i - E_0). \tag{9}$$

3 Results and discussion

In this section we present and analyze the numerical results for n-type ADDDQWs in the presence of electromagnetic fields. Firstly, we obtain the energies and squared wave functions of the lowest four subband levels in the confinement potential by taking into account the effect of electric and magnetic fields. Then we focus on the calculation of NOR, SHG and THG coefficients as functions of incident photon energies considering the energy transitions between ISB levels. The set of parameters used in the numerical simulation are $m^* = 0.067 m_0$ (where m_0 is the free electron mass), $L_w = 150$ Å , $\Gamma_1 = 1.0$ THz , $\Gamma_2 = 5.0$ THz, and $\Gamma_3 = 7.0$ THz. The ionized impurity density in the left-side QW is 3×10^{12} cm^{-2} and in the right-side QW is 7×10^{12} cm^{-2}.

Figure 1 shows the confining potential profiles and first four bound state energy levels and their associated squared wave functions in the ADDDQWs of the above-mentioned configuration in the absence and in the presence of applied electromagnetic fields. Figure 1a depicts the confinement potential without any external fields. Due to the different doping impurity levels the potential is clearly asymmetric and as a result of higher densities in the right-side well, the right potential well is deeper.

In Fig. 1b we present the effect of in-growth static electric field on the potential profile, energy levels and squared wave functions. Electric field modifies the confinement potential by changing the shape of its profile. It significantly bends the left side of potential. The degree of confinement at the negative zone of spatial region weakens, while the positive zone becomes more. For handled asymmetric δ-doped QW the impact of electric field is slighter at the bottom of the confinement potential but it strengthens at the upper region of the potential. The energy levels change as a result of the alterations in the confinement potential. The shift of the ground states energy level towards a higher energy is visible. Clearly, the influence of the electric field is more pronounced for the case of the squared

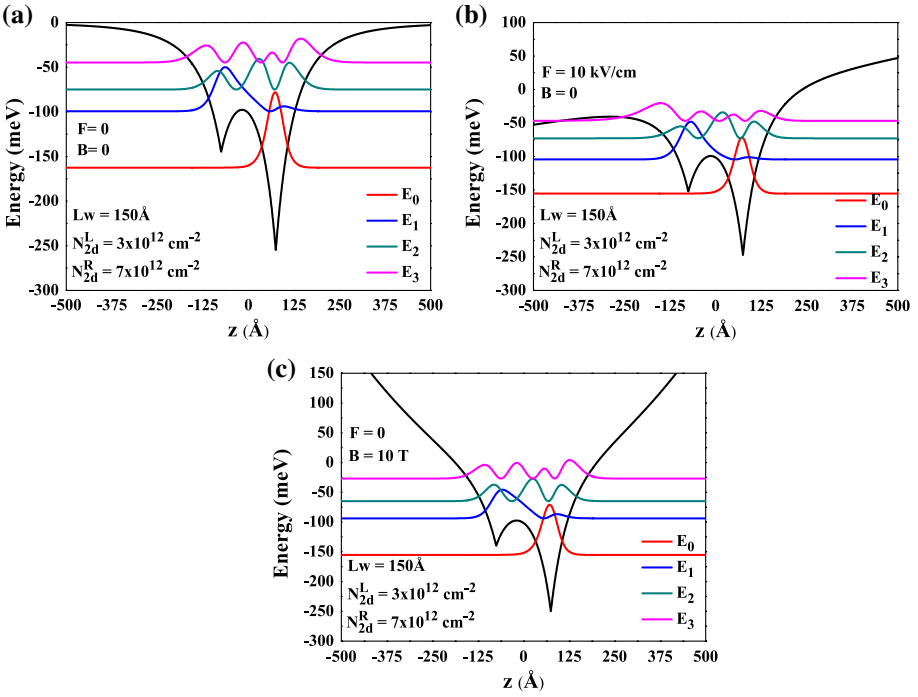


Fig. 1 The position dependency of confining potential (solid black line) and the energies of the first four subband energy levels together with their corresponding squared wave functions (colored solid lines) in the asymmetrical double n-type δ-doped quantum well: **a** without electromagnetic fields, **b** with electric field, **c** with magnetic field

wave function of the fourth energy level because of the strong modifications in the confinement potential at its vicinity.

The squared wave functions of the lowest three levels are less affected by the presence of the applied electric field, and one may observe a decreasing of their amplitudes within the QW region, related with the loss in electron localization.

To make the effect of electric field on the energy differences between sublevels and squared wave functions of these levels clearer, we present the Table 1. Second column of Table 1 gives the energy difference between first excited state and ground state ($E_{10} = E_1 - E_0$). Second and third columns are the half and third parts of the transition

Table 1 First three columns introduce the transition energies from the ground state to the first, second, and third excited states, respectively; for three electric field values. Last three columns represent the variation in the values of the products of dipole moment matrix elements as needed for evaluating NOR, SHG and THG coefficients, respectively

	E_{10} (meV)	$\frac{1}{2}E_{20}$ (meV)	$\frac{1}{3}E_{30}$ (meV)	M^2_{01}(Å^2)	$M_{01}M_{12}M_{20}$(Å^3)	$M_{01}M_{12}M_{23}M_{30}$(Å^4)
$F = 0$ (kV/cm)	63.167	43.749	39.266	27,598	15,389	237,515
$F = 5$ (kV/cm)	57.250	42.624	38.177	26,419	13,517	307,025
$F = 10$ (kV/cm)	51.013	41.291	36.210	26,703	12,347	323,102

energies between the ground state and the second and third exited states, respectively, suitable for the evaluation of SHG and THG coefficients. Last three columns of Table 1 show the values of the factors containing dipole moment matrix elements, as they appear in the expressions (4–6), related to NOR, SHG and THG coefficients, respectively. As seen from the Table 1, the increase in the electric field intensity produces a reduction of the resonant transition energies, with the more pronounced effect taking place in the case of E_{10}. On the other hand, the changes in the wave functions, especially the spatial overlap between them, reveal themselves in the behavior of the dipole moment matrix elements. Accordingly, the squared off-diagonal matrix element, related with the main transition, M_{01}^2, shows a steady decrease as long as the growing electric field allows the extension of the first excited state wave function towards negative values of the z-coordinate. Furthermore, this feature also affects the value of the product $M_{01}\, M_{12}M_{20}$, which also shows a diminishing trend, whereas the product $M_{01}M_{12}M_{23}M_{30}$, on the contrary, undergoes a significant increment due to the rise in the spatial overlap between the wave functions of upper states within the negative region of the coordinate.

The influence of in-plane applied magnetic field on the confinement potential profile, energy levels and the corresponding squared wave functions is displayed in the Fig. 1c. The magnetic field makes the confinement potential stronger without breaking the asymmetry. Although the magnetic field leads to small perturbations at the bottom of the potential, it causes significant impact at the upper part of potential by increasing the height of potential barriers. The effect of magnetic field not only shifts to ground state energy level but also shifts the exited states energy levels to the higher energies. With the increment of the magnetic field intensity, the overlap between the states slightly increase with the sole exception of the states $\phi_0(z)$ and $\phi_2(z)$, for which the off-diagonal matrix element M_{20} exhibits a reduction that causes the overall decreasing of $M_{01}M_{12}M_{20}$. Table 2 displays the numeric values of the transition energies between excited states and ground state, and the dipole moment matrix elements related to these states in the presence of magnetic field.

By taking into consideration the electronic properties we examine the optical properties of ADDDQW with applied electric and magnetic fields. Figure 2a shows the variation of NOR coefficient versus the incident photon energy for several electric field values. The peak positions of NOR coefficients move to the lower energies with greater values of electric field. Such a tendency could be expected from the field-induced decrease in the main transition energy, E_{10}. Peak amplitudes decrease linearly due to decrement in M_{01}^2 for increasing electric field strength. In Fig. 2b we depict the influence of magnetic field on the NOR response as a function of incident photon energy. The application of magnetic field results in a reverse behavior of NOR coefficient, compared to that shown under the influence of an electric field. Peak positions shift to the higher energies (blue-shift), showing at the same time a rise in peak amplitudes with the increment of the magnetic field. Such

Table 2 First three columns introduce the transition energies between first, second, third exited states and ground state, respectively; last three columns represent the variation in the values of the products of dipole moment matrix elements as needed for evaluating NOR, SHG and THG coefficients, respectively, for three magnetic field values

	E_{10} (meV)	$\frac{1}{2}E_{20}$ (meV)	$\frac{1}{3}E_{30}$ (meV)	M_{01}^2(Å^2)	$M_{01}M_{12}M_{20}$(Å^3)	$M_{01}M_{12}M_{23}M_{30}$(Å^4)
$B = 0$ (T)	63.167	43.749	39.266	27,598	15,389	237,515
$B = 10$ (T)	66.149	45.139	42.755	30,660	15,059	359,948
$B = 20$ (T)	70.228	47.092	48.741	40,274	14,547	409,273

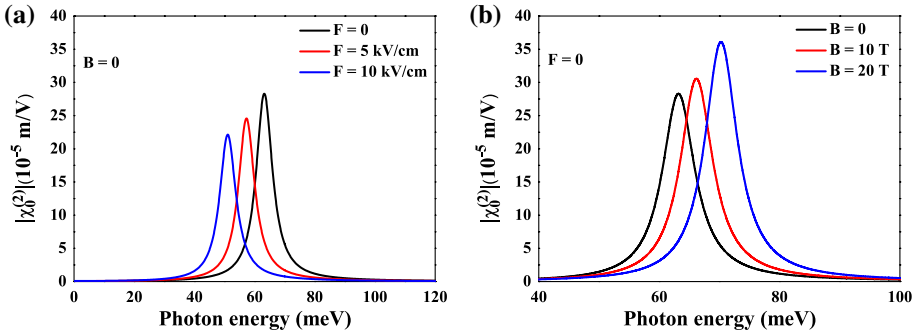


Fig. 2 The variation of the coefficient of nonlinear optical rectification as a function of the incident photon energy in an asymmetric double δ-doped quantum well, for three different values of electric field (**a**), magnetic field (**b**)

blue-shift of resonance peaks is consistent with the study of Martínez-Orozco and coworkers (2017).

In Fig. 3a, b we plot the SHG coefficient as a function of incident photon energy in the presence of an electric and a magnetic field, respectively. Figure 3a presents a main resonant peak corresponding to the $E_{20}/2$ transition energy and a secondary peak corresponding to E_{10} transition energy. It is possible to notice that the two-resonance structure of SHG coefficient starts to vanish at higher field values such as $F = 10$ kV/cm and $B = 20$ T. The main reason for that is that the resonant peak associated to E_{20} spreads over a wide range of incident photon energy and suppresses the appearing of secondary peak of E_{10}. The closeness of the $M_{01}M_{12}M_{20}$ dipole matrix element values when the fields are applied also affects the configuration of SHG peaks. Although the main peak positions of SHG slightly move to the lower energies with the effect of electric field, they slightly move to higher energies with the effect of magnetic field as concluded in the paper of Martínez-Orozco et al. (2017). The main peak amplitudes are enhanced with greater values of both electric and magnetic field.

Lastly, we investigate the influence of applied electric and magnetic fields on the THG coefficients. Figure 4a presents the THG behavior against incident photon energy

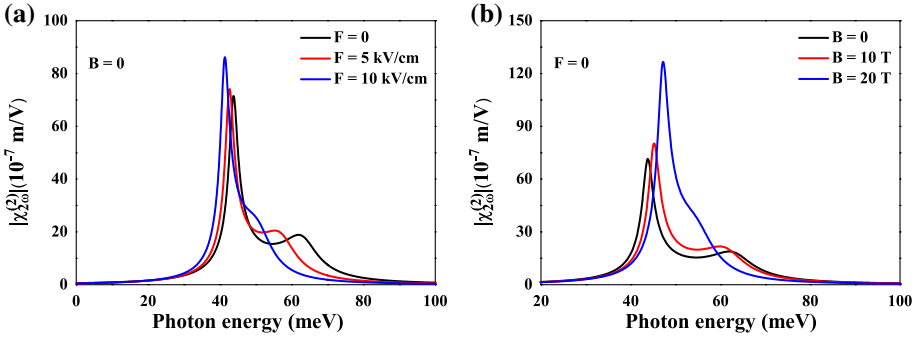


Fig. 3 The variation of the coefficient of second harmonic generation versus incident photon energy in an asymmetric double δ-doped quantum well, for three different values of electric field (**a**), magnetic field (**b**)

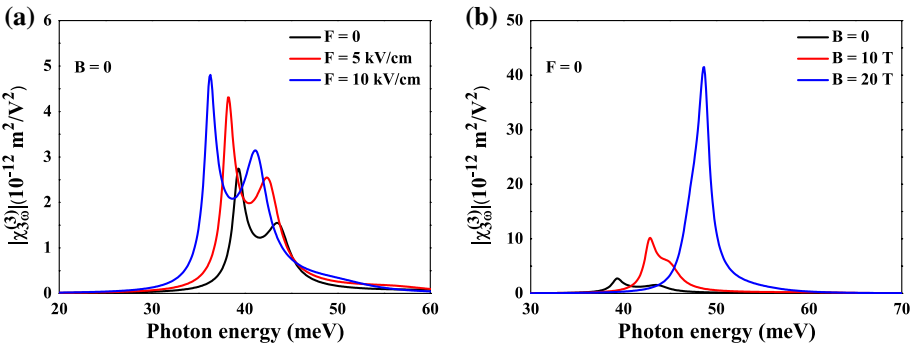


Fig. 4 The change of the coefficient of third harmonic generation as a function of incident photon energy in an asymmetric double δ-doped quantum well, for three different values of electric field (**a**), magnetic field (**b**)

with electric field. Main and secondary peaks corresponding to $E_{30}/3$ and $E_{20}/2$, respectively, can be seen but tertiary peaks corresponding to E_{10} are absent for all studied electric field values. With the strengthening of the electric field, the main peak positions of THG move to lower photon energies by increasing their peak amplitudes. Figure 4b shows the variation of THG coefficients versus incident photon energy with the effect of magnetic field. A feeble secondary peak comes into sight only at zero magnetic field, although territory peaks completely disappear in the applied and also the non-applied magnetic field condition. The main reason for the vanishing secondary peaks is the superposition of the main and secondary resonant peaks of THG coefficient due to closeness of transition energies $E_{30}/3$ and $E_{20}/2$ whose values are given in Table 2. On the other hand the reason for the suppression of tertiary peaks can be explained as clarified by Martínez-Orozco et al. (2017). The resonant peak at the incident photon energies $\hbar\omega = E_1 - E_0$ is lower enough to being suppressed with the product of energy term $\hbar^2(2\omega - \omega_{20} - i\Gamma_3)(3\omega - \omega_{30} - i\Gamma_3)$ given in the denominator of THG coefficient (Martínez-Orozco et al. 2017).

The main peak positions of THG move to higher energies (blue-shift) by enhancing their amplitudes when magnetic field is increased. That blue-shift behavior of resonance peaks is again consistent with the study of Martínez-Orozco et al. (2017). The shift to higher energies and the increment in the main peak amplitudes with increasing magnetic field are attributed to the increase in the energy transitions of $E_0 \rightarrow E_3$ and the rise in the product of dipole moment matrix elements $M_{01}\,M_{12}M_{23}M_{30}$, respectively.

Before ending the discussions on the influence of magnetic fields on the NOR, SHG and THG coefficients it is essential to talk about the Zeeman splitting. In that study magnetic field is applied perpendicularly to the growth direction. Hence the influence of magnetic field can be pronounced in the confining potential by leading it parabolic form. The in-plane magnetic fields do not cause Zeeman splitting so the extra energy levels in the QW. Thus we can conclude that coefficients of NOR, SHG and THG are not affected from in-plane magnetic field. We can also point out that if the magnetic field being applied in the growth direction the effect of Zeeman splitting on the stated coefficients will be so little as a consequence of roughly hundred times smaller splitting energy values compared to the transition energies.

4 Conclusion

We have performed a theoretical investigation on the behavior of nonlinear optical rectification, second and third harmonic generation coefficients in an asymmetric double δ-doped quantum well subjected to the external electric field and magnetic field. Bound states have been considered in order to analyze the optical properties. Results show that the positions of the resonant peaks of NOR, SHG and THG versus incident photon energy exhibit a red-shift (blue-shift) with increment in electric (magnetic) field. The presented results indicate that the peak locations and magnitudes of the optical coefficients could be tuned by applying electric and magnetic field. The results could be helpful for the studies based on the nonlinear optical properties in the δ-doped structures.

Acknowledgements MEMR thanks Universidad de Medellín for hospitality and support during 2019–2020 sabbatical stay. He also acknowledges Mexican Conacyt for partial support through research Grant No. A1-S-8218 (CB 2017-2018), and SEP-PRODEP for support through "Estancias Cortas" fellowship.

References

Baskoutas, S., Paspalakis, E., Terzis, A.F.: Electronic structure and nonlinear optical rectification in a quantum dot: effects of impurities and external electric field. J. Phys. Condens. Matter **19**, 395024 (2007)

Chen, B., Guo, K.-X., Wang, R.-Z., Zheng, Y.-B., Li, B.: Nonlinear optical rectification in asymmetric double triangular quantum wells. Eur. Phys. J. B **66**, 227–233 (2008)

Chen, T., Xie, W., Liang, S.: The nonlinear optical rectification of an ellipsoidal quantum dot with impurity in the presence of an electric field. Physica E **44**, 786–790 (2012)

Dakhlaoui, H., Nefzi, M.: Tuning the linear and nonlinear optical properties in double and triple δ-doped GaAs semiconductor: impact of electric and magnetic fields. Superlattices Microstruct. **136**, 106292 (2019)

Ganguly, J., Saha, S., Pal, S., Ghosh, M.: Fabricating third-order nonlinear optical susceptibility of impurity doped quantum dots in the presence of Gaussian white noise. Opt. Commun. **363**, 47–56 (2016)

Giraldo-Tobon, E., Ospina, W., Miranda-Pedraza, G.L., Mora-Ramos, M.E.: Influence of applied electric fields on the electron-related second and third-order nonlinear optical responses in two dimensional elliptic quantum dots. Superlattices Microstruct. **83**, 157–167 (2015)

Guo, K.-X., Gu, S.-W.: Nonlinear optical rectification in parabolic quantum wells with an applied electric field. Phys. Rev. B **47**, 16322–16325 (1993)

Guo, K.-X., Chen, C.-Y., Das, T.P.: Studies on the third-harmonic generation of double-layered quantum wires in magnetic fields. Opt. Quantum Electron. **33**, 231–237 (2001)

Ioriatti, L.: Thomas-Fermi theory of 5-doped semiconductor structures: exact analytical results in the high-density limit. Phys. Rev. B **41**, 8340–8344 (1990)

Karabulut, I., Safak, H.: Nonlinear optical rectification in semiparabolic quantum wells with an applied electric field. Physica B **368**, 82–87 (2005)

Karabulut, I., Mora-Ramos, M.E., Duque, C.A.: Nonlinear optical rectification and optical absorption in GaAs–Ga1–xAlxAs asymmetric double quantum wells: combined effects of applied electric and magnetic fields and hydrostatic pressure. J. Lumin. **131**, 1502–1509 (2011)

Karimi, M.J., Keshavarz, A.: Second harmonic generation in asymmetric double semi-parabolic quantum wells: effects of electric and magnetic fields, hydrostatic pressure and temperature. Physica E **44**, 1900–1904 (2012)

Kirak, M., Altinok, Y.: The electric field effects on the third-harmonic generation in spherical quantum dots with parabolic confinement. Eur. Phys. J. B **85**, 344 (2012)

Kozuka, Y., Kim, M., Ohta, H., Hikita, Y., Bell, C., Hwang, H.Y.: Enhancing the electron mobility via delta-doping in SrTiO3. App. Phys. Lett. **97**, 222115 (2010)

Li, B., Guo, K.-X., Zhang, C.-J., Zheng, Y.-B.: The second-harmonic generation in parabolic quantum dots in the presence of electric and magnetic fields. Phys. Lett. A **367**, 493–497 (2007)

Li, B., Guo, K.-X., Liu, Z.-L., Zheng, Y.-B.: Nonlinear optical rectification in parabolic quantum dots in the presence of electric and magnetic fields. Phys. Lett. A **372**, 1337–1340 (2008)

Li, X., Zhang, C., Tang, Y., Wang, B.: Nonlinear optical rectification in asymmetric quantum dots with an external static magnetic field. Physica E **56**, 130–133 (2014)
Liu, X., Zou, L., Liu, C., Zhang, Z.-H., Yuan, J.-H.: The nonlinear optical rectification and second harmonic generation in asymmetrical Gaussian potential quantum well: effects of hydrostatic pressure, temperature and magnetic field. Opt. Mater. **53**, 218–223 (2016)
Liu, G., Guo, K., Zhang, Z., Hassanbadi, H., Lu, L.: Electric field effects on nonlinear optical rectification in symmetric coupled $Al_xGa_{1-x}As/GaAs$ quantum wells. Thin Solid Films **662**, 27–32 (2018)
Martínez-Orozco, J.C., Rodríguez-Magdaleno, K.A., Suárez-López, J.R., Duque, C.A., Restrepo, R.L.: Absorption coefficient and relative refractive index change for a double δ-doped GaAs MIGFET-like structure: electric and magnetic field effects. Superlattices Microstruct. **92**, 166–173 (2016)
Martínez-Orozco, J.C., Rojas-Briseño, J.G., Rodríguez-Magdaleno, K.A., Rodríguez-Vargas, I., Mora-Ramos, M.E., Restrepo, R.L., Ungan, F., Kasapoglu, E., Duque, C.A.: Effect of the magnetic field on the nonlinear optical rectification and second and third harmonic generation in double δ-doped GaAs quantum wells. Physica B **525**, 30–35 (2017)
Mora-Ramos, M.E., Duque, C.A., Kasapoglu, E., Sari, H., Sokmen, I.: Linear and nonlinear optical properties in a semiconductor quantum well under intense laser radiation: effects of applied electromagnetic fields. J. Lumin. **132**, 901–913 (2012)
Ozturk, E.: Optical intersubband transitions in double Si δ-doped GaAs under an applied magnetic field. Superlattices Microstruct. **46**, 752–759 (2009)
Panda, S., Das, T., Panda, B.K.: Nonlinear optical susceptibilities in $In_xGa_{1-x}N/GaN$ hexagonal single quantum well under applied electric field. Superlattices Microstruct. **135**, 106238 (2019)
Restrepo, R.L., Kasapoglu, E., Sakiroglu, S., Ungan, F., Morales, A.L., Duque, C.A.: Second and third harmonic generation associated to infrared transitions in a Morse quantum well under applied electric and magnetic fields. Infrared Phys. Technol. **85**, 147–153 (2017)
Rezaei, G., Karimi, M.J.: Third harmonic generation in a coaxial cylindrical quantum well wire: magnetic field and geometrical size effects. Opt. Commun. **285**, 5467–5471 (2012)
Rodíguez-Magdaleno, K.A., Martínez-Orozco, J.C., Rodríguez-Vargas, I., Mora-Ramos, M.E., Duque, C.A.: Asymmetric GaAs n-type double δ-doped quantum wells as a source of intersubband-related nonlinear optical response: effects of an applied electric field. J. Lumin. **147**, 77–84 (2014)
Rosencher, E., Bois, P.: Model system for optical nonlinearities: asymmetric quantum wells. Phys. Rev. B **44**, 11315–11327 (1991)
Rosencher, E., Bois, P., Nagle, J., Costard, E., Delaitre, S.: Observation of nonlinear optical rectification at 10.6 μm in compositionally asymmetrical AlGaAs multiquantum wells. Phys. Lett. **55**, 1597–1599 (1989)
Shao, S., Gou, K.X., Zhang, Z.H., Li, N., Peng, C.: Third-harmonic generation in cylindrical quantum dots in a static magnetic field. Solid State Commun. **151**, 289–292 (2011)
Tsang, L., Ahn, D., Chuang, S.L.: Electric field control of optical second harmonic generation in a quantum well. Appl. Phys. Lett. **52**, 697–699 (1988)
Vaseghi, B., Sadri, M., Rezaei, G., Gharaati, A.: Optical rectification and third harmonic generation of spherical quantum dots: controlling via external factors. Physica B **457**, 212–217 (2015)
Wang, G.: Third-harmonic generation in cylindrical parabolic quantum wires with an applied electric field. Phys. Rev. B **72**, 155329 (2005)
Xia, J.-B., Fan, W.-J.: Electronic structures of superlattices under in-plane magnetic field. Phys. Rev. B **40**, 8508–8515 (1989)
Yıldırım, H., Tomak, M.: Nonlinear intersubband optical absorption of Si δ-doped GaAs under an electric field. Phys. Stat. Sol. (b) **243**, 2874–2881 (2006)
Yu, Y.B., Wang, H.J.: Third-harmonic generation in two-dimensional pseudodot system with applied magnetic field. Superlattice Microstruct. **50**, 252–260 (2011)
Zhang, L., Xie, H.-J.: Electric field effect on the second-order nonlinear optical properties of parabolic and semiparabolic quantum wells. Phys. Rev. B **68**, 235315 (2003)
Zhang, L., Xie, H.-J.: Bound states and third-harmonic generation in a semi-parabolic quantum well with an applied electric field. Physica E **22**, 791–796 (2004)
Zhang, Z.-H., Guo, K.-X., Chen, B., Wang, R.-Z., Kang, M.-W.: Nonlinear optical rectification in cubical quantum dots. Phys. B Condens. Matter **404**, 2332–2335 (2009a)
Zhang, Z.-H., Guo, K.-X., Chen, B., Wang, R.-Z., Kang, M.-W.: Third-harmonic generation in cubical quantum dots. Superlattices Microstruct. **46**, 672–678 (2009b)

Publisher's Note Springer Nature remains neutral with regard to jurisdictional claims in published maps and institutional affiliations.